We are IntechOpen,
the world's leading publisher of
Open Access books
Built by scientists, for scientists

6,900
Open access books available

186,000
International authors and editors

200M
Downloads

154
Countries delivered to

Our authors are among the

TOP 1%
most cited scientists

12.2%
Contributors from top 500 universities

CLARIVATE ANALYTICS
BOOK CITATION INDEX
INDEXED

WEB OF SCIENCE™

Selection of our books indexed in the Book Citation Index
in Web of Science™ Core Collection (BKCI)

Interested in publishing with us?
Contact book.department@intechopen.com

An Investigation of an Acoustic Wave Velocity in a Reinforced Concrete Beam from Out-of Plane and in Plane Sources

Noorsuhada Md Nor, Norazura Muhamad Bunnori, Azmi Ibrahim,
Hamidah Mohd Saman, Shahiron Shahidan and Soffian Noor Mat Saliah

Additional information is available at the end of the chapter

http://dx.doi.org/10.5772/54448

1. Introduction

Acoustic Emission (AE) is a phenomenon of a transient stress waves resulting from a sudden release of elastic energy, caused by mechanical deformations, initiation and propagation of microcracks, dislocation movement, and other irreversible changes in material [1]. AE sensors are used to detect the acoustic waves at the surface of a structure, produced by AE events either on the surface or in the bulk of the material [2].

There are two types of signals in the AE system; namely burst and continuous signals. Burst signal is a separate type of signal of a very short duration (in the range of a few microseconds (µs) to a few miliseconds (ms)) and it is a broad frequency domain spectrum. Meanwhile the continuous signal is emitted close to each other or the burst is very high rate. The continuous signal is also occurred very close and sometimes overlaps. When the AE signal or output is transmitted in a structure, an array is identified. The output is always represented in a waveform which has information on a source location. A key to compute a source location is by determination of the wave velocity of the wave propagation. If incorrect wave velocity was used either owing to poor assumption or triggering of the system, it would affect to the determination of the source location [3]. Thus accurate wave velocity is important for the determination of the source location prior to any AE test.

The AE wave velocity can be determined by estimating the time of arrival (TOA) of the wave propagating in the structure; normally based on the threshold level [3] or frequency [4]. Typically, the propagation of wave in concrete can be categorized into three different types; namely dilatation wave (compression waves, longitudinal wave or P-wave for primary), the distortion wave (shear waves or S-wave for secondary) and the Rayleigh wave

(surface wave or R-wave) [5–7]. Longitudinal wave is known as L – wave or P – wave; which the wave travels in the material and Rayleigh wave (R-wave) travels along the surface of the specimen. The initiation time of the P-wave is when the first TOA of the elastic wave reaches to each sensor. If the onset of the S-wave is detected, this information can be used either in combination with P-wave or be considered as P-wave onset [8]. Determining S–wave is challenging because the distance between sensor and receiver is only few wavelengths. Another problem is because the onset of the S–wave is hidden in the P–wave [8]. Generally, an S-wave is normal to the direction of the wave propagation and a P-wave, parallel. Determination of onset time can be done visually or automatically. This depends on the onset definition itself and also by picking algorithm. In relation with the wave velocity, the P-wave travels at a higher velocity than S-wave [9]. In concrete, the S-wave velocity is approximately 40% less than of the P-wave velocity and R-wave velocity is 92 % of the S-wave velocity and 56 % of the P-wave velocity [10]. However, only the P-wave would be considered in this study based on the TOA.

In order to determine the wave velocity, AE signals are produced by pencil lead fracture (PLF), known as Hsu-Nielsen technique. In this technique, PLF is the monopoles which is normally applied to the outside of the test sample, and the real AE signal is nearly dipoles in which the AE sources that originated from the points are buried inside the sample [11]. The previous PLF was used to generate simulated acoustic emission signals in an aluminum plate at different angles; 0, 30, 60 and 90 degree with respect to the plane of the plate [12]. Next, it is suggested that the plate wave analysis be used to determine the source orientation of acoustic emission sources. A few researchers have used the same method in the heterogeneous material as well as reinforced concrete (RC) [3, 13]. To verify the wave velocity propagation in the RC beam, corrected signal was used by Muhamad Bunnori [3], by normalizing each signal for peak value of amplitude up to 10 volts. The same method was also utilized for this analysis.

In this study, various threshold levels were performed to determine the TOA and the wave velocity in the RC beams with shorter source-to-sensor distance. Very little attention has been given on the shorter distance between sensor and sensor to source distance. An AE source was specified and focused on out-of plane and in-plane of the arrangement of sensor faces. Three main objectives are addressed. Firstly to study the relationship between wave velocity and sensor distance, secondly to investigate the relationship between wave velocity and threshold level and lastly to observe the relationship between arrival time and sensor distance.

2. Experimental procedure

2.1. Preparation of beam specimen

The test of wave velocity was carried out on a reinforced concrete (RC) beam with dimension of 150 mm x 150 mm x 750 mm; designed in accordance with British Standard [14] for grade C40. The concrete was made up from cement, water, fine aggregate and coarse aggregate with proportion of 1: 0.43: 2.16: 2.60, respectively. Then, 1 % of water reducer

agent (Rheobuild 1100) of cement weight was added in the concrete mix to improve the workability of the fresh concrete. The maximum coarse aggregate of 20 mm was used.

The beams were designed as a singly RC beam with two high yield steels of 16 mm to strengthen the tension part and two mild steels of 8 mm as hanger bars. The bars were bent at both end to form a standard hook of 60 mm at tension part and 30 mm at compression part. In the stirrups, 12 diameter of mild steel with spacing of 100 mm centre to centre was used. In the preparation of each RC beam, the reinforcement was submerged in the standard mould of 150 mm x 150 mm x 750 mm with cover of 20 mm, before the concrete mix was cast. All beams were demoulded after ±24 hours and submerged in the water curing tank for 28 days. In order to ensure the design fulfilled the strength, the cubes were prepared and tested under compression test for 7 and 28 days. The compressive strength for 7 days was found to be 32.35 N/mm^2 and 44.65 N/mm^{2}at age of 28 days.

2.2. Acoustic emission system

Acoustic emission (AE) was monitored using a MicroSAMOS (μSAMOS) supplied by Physical Acoustic Corporation (PAC). The system consists of integral preamplifier acoustic emission sensors (transducers) R6I (40 – 100 kHz); a notebook acoustic emission system board (8 (channels) x 16 (hubs) bit acoustic emission channels, low peak and high peak filters, 2 MHz bandwidth, auto sensor test (AST), time definition display (TDD), digital signal processor (DSP) and waveform module; personal computer memory card international association (PCMCIA) interface card; cables; internal and external parametric cable set; a notebook personal computer with full suite of AEWin Software; universal serial bus (USB) license key; and magnetic clamps. The acquisition parameters in the AEWin software were summarized in Table 1.

Parameter	Value
Hit definition time (HDT)	2000μs
Peak definition time (PDT)	1000μs
Hit lockout time (HLT)	500μs
Preamplifier (R6I)	40dB
Bandpass data acquisition filter	400kHz
Sample rate	100ksps
Analog filter (lower)	1kHz
Pre-trigger	250,000

Table 1. AE test parameters

2.3. AE sensor installation and sensitivity checking

Prior to the wave velocity test, three pairs of thin plates were prepared to attach the sensors S1, S2 and S3 with the distance of 200 mm and 100 mm between pair of plates. Spacing between two plates is 45 mm. The beam surface was polished smoothly using course sand

paper to ensure good connectivity between sensors and beam surface. The plates were then fixed to the beam surface using epoxy and hardener.

Three sensors were coupled on the beam surfaces at the selected point using a good couplant such as a thin layer of high performance grease. The thinnest practical layer of couplant is usually the best [15]. The magnetic clamps were used to safeguard the sensors; which sensors held in position in magnetic clamps; then the magnetic clamps properly coupled to the steel plates.

With sensors in good mounting condition, calibration (sensitivity) checking was carried out to recognize the sensitivity of the sensors. In this experiment, a magnetic pencil with a Nielson shoe (Teflon shoe) was used to break a 0.5 mm 2 H lead to generate a simulated acoustic wave against the surface of the beam. The handling method of the magnetic pencil has been presented in ASTM E976 [16]. All sensors would significantly coupled if the wave was generated by at least three or more replicates of pencil lead fracture (PLF). This might produce high amplitude of 99 dB or the sensitivity within ± 3 dB in different [3, 17]. Based on the research done by others, it was found that the amplitude recorded by each sensor should not be permitted to vary more than 4 dB from the average of all sensors [18]. This technique was used to ensure that the sensor and the beam were in a good contact to provide an adequate result throughout the test. If these criteria are not met, the sensors on the beam surface would be remounted and sensitivity check was carried out until the amplitude fulfilled the requirement.

2.4. Wave velocity test

In this experimental work, three integral preamplifier R6I sensors with 55 kHz resonant frequency were used. Acoustic emission sensors are transducers that convert the mechanical waves into electrical signal [19], where the information about the existence and location of possible damage or stress released sources can be obtained. The specification and feature of the sensor is shown in Table 2.

Specification	Value
Dimension (Ø x height) mm	29 x 40
Weight (gm)	98
Operating temperature ($0^{o}c$)	-45 to +85
Shock limit (g)	500
Peak sensitivity (V/m/s)	120
Directionality (dB)	+1.5

Table 2. Specification and feature of the R6I sensor

A schematic diagram of the test set up for beam size of 150 mm x 150 mm x 750 mm and 100 mm x 100 mm x 500 mm in a linear structure is shown in Figure 1 and Figure 2, respectively. The AE sources were identified on the out-of plane and in plane of the sensors arrangement or source parallel to the sensor face. Three sensors were mounted in a symmetrical

arrangement on the RC beam using a thin layer of high vacuum grease as a couplant with the same spacing of 200 mm centre to centre for beam 150 mm x 150 mm x 750 mm and 100 mm centre to centre for beam 100 mm x 100 mm x 500 mm.

In this experiment, four different pre-set threshold levels were chosen namely 40 dB, 45 dB, 65 dB and 70 dB. At each threshold level, 15 replicates of PLF were applied to generate a simulated AE source at the same spot or the same AE source location. When the lead is pressed against the RC beam surface, the applied force produces a local deformation and the stress where the lead touched is suddenly being released. It is important to handle the pencil properly while breaking the lead against the testing specimen to get significant value. Improper handling of the pencil would give imprecise value; which will affect the TOA. The proper breaking of the lead creates a very short-duration, localized impulse that is quite similar to a natural acoustic emission source such as crack [19]. The lead was extended to 0.1 inches and the pencil was slanted down 30^0 to the plane of the beam surface, as suggested by other researchers [18, 20]. The out-of plane AE source was located at the centre of the cross section of the end beam. As for in-plane AE source, it was located at 100 mm from Sensor 1 as illustrated in Figures 1 and 2.

In the AE hardware, for in-plane source, Sensor 1 was set as individual and the rest were synchronized. Meanwhile, for out-of plane source, Sensor 3 was set as individual and the rest were synchronized. The same method applied for beam size of 100 mm x 100 mm x 500 mm.

In acoustic emission, waveform parameters normally used are frequency and amplitude [22]. Amplitude of AE signal parameter was used in identification of wave velocity. It is defined as the magnitude of the peak voltage of the largest excursion attained by the signal waveform from single emission event [1]. Amplitude is reported in decibels (dB) to measure signal size and typical AE signal is represented as a voltage versus time curve. Voltage is converted to dB using the following equation:

$$A = 20 \log (V/V_{ref}) \tag{1}$$

Where: A is an amplitude (dB), V is voltage of peak excursion and V_{ref} is the reference voltage. Generally the dB scale runs from 0 to 100 [21]; which depend on the threshold set.
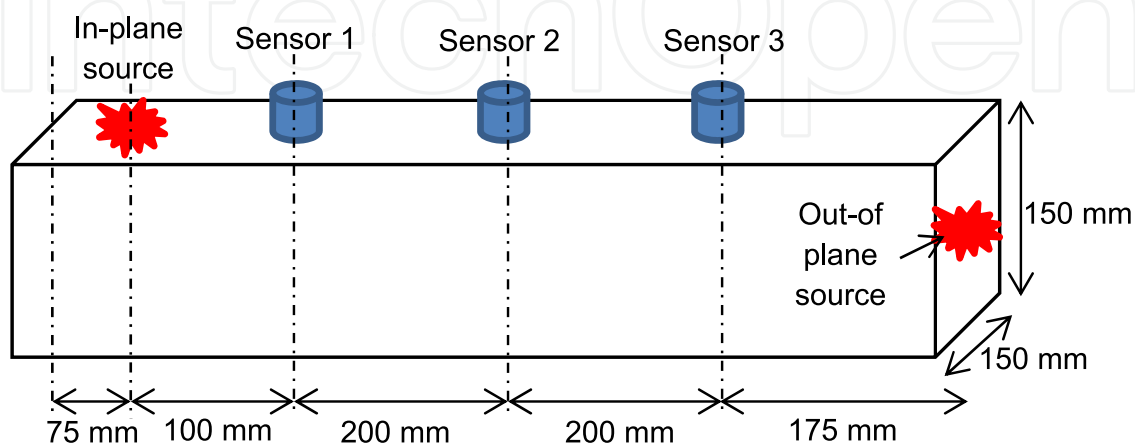

Figure 1. Schematic diagram of sensors location on the RC beam 150 mm x 150 mm x 750 mm
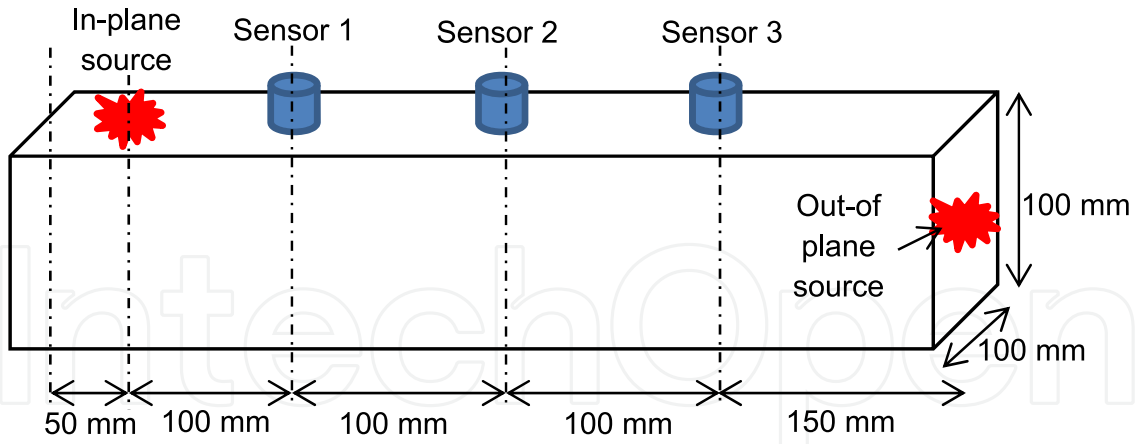
Figure 2. Schematic diagram of sensors location on the RC beam 100 mm x 100 mm x 500 mm

In a relationship between threshold level and amplitude, preamplifier was considered; where equation (2) was used to calculate amplitude:

$$\text{Threshold} = \text{Amplitude} - \text{Preamplifier} \qquad (2)$$

The rudimentary determination for location calculation is based on time-distance relationship implied by the velocity of the sound wave [4, 23]; where the absolute arrival time, t, of a hit in an event combine with the velocity, v (v is P-wave velocity [19]), of the sound wave to yield the distance, d, from sensor to the source as represented by

$$d = v\,t \qquad (3)$$

Generally the distance between the two sensors depends on the geometry of the sample. Determination of TOA (the exact time the event originated) was made by recording many data hits for each AE event. t_1 represents the time of arrival (or arrival of longitudinal wave, P-wave) at Channel 1. Meanwhile t_2 is arrival of P-wave at Channel 2. The arrival time difference between the arrivals of the signal at the two sensors can be written as

$$\Delta T = (t_1 - t_2) \qquad (4)$$

At selected source locations (either out-of plane or in-plane), 10 replicates of PLF were applied from the lower threshold level of 40 dB to the higher 70 dB. Distance for beam 150 mm x 150 mm x 750 mm from sensors 1-2 and sensors 1-3 is 200 mm and 400 mm, respectively. Meanwhile, for beam 100 mm x 100 mm x 500 mm, the distance from sensors 1 to 2 is 100 mm and sensors 1 to 3 is 200 mm.

The relationship between wave velocity and threshold level, and TOA and sensor distance were correlated. Both correlations were then verified by corrected AE signal. Corrected AE signal was used for a particular threshold level, the same temporal position in each waveform which involves the normalizing of each signal up to a peak value of 10 volts. In this research, the corrected signal was used for the evaluation of TOA for each threshold level. The corrected signal can be identified by normalizing the peak signal of a hit to 10 volts followed by other signal in a hit. Then, the TOA for each threshold was then determined.

3. Results and discussion

3.1. Sensitivity checking

Sensitivity checking was used to ensure the sensor and the beam was in a good contact to provide an adequate results. The sensors must have a higher sensitivity [24] in order to get good contact between sensors surface and beam surfaces. In this experimental in order to check the sensitivity, at least ten numbers of 99 dB were considered for each sensor. The responses of the transducer to PLFs are shown in Figure 3. Sensor 1 represents a good sensitivity since almost of all the PLFs produced amplitude of 99 dB. However, Sensor 2 needs several trials to ensure the sensors and the beam surface have a good contact. These scenarios that occurred in Sensors 1 and 2 are related with the signal waveform produced from the PLF. It is typically affected by the source characteristics, the path taken from the source to the sensors, the characteristic of the sensor and the measurement system [25]. The waveform for Hit 1 and Hit 12 are represented in Figure 4.
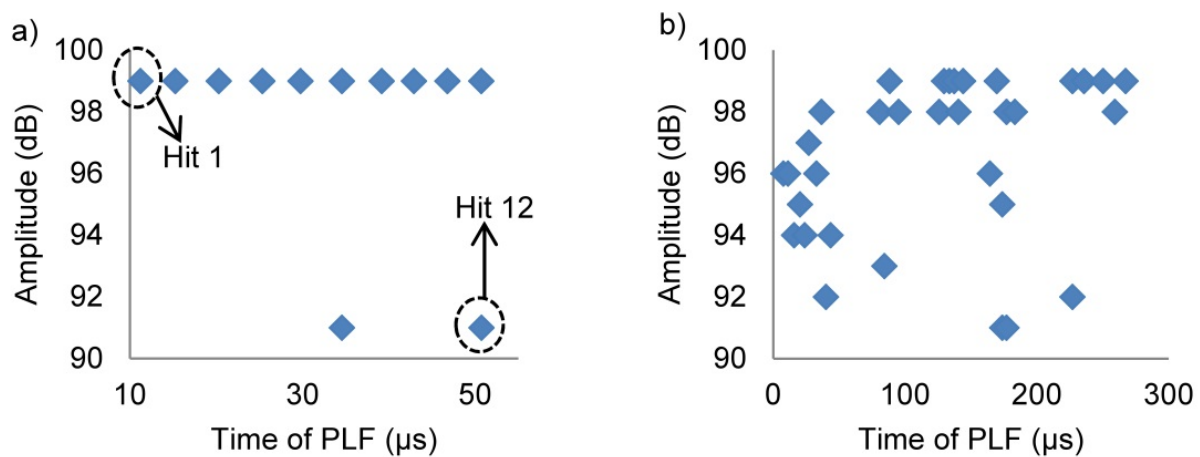

Figure 3. Response to PLF on reinforced concrete beam for a) Sensor 1 and b) Sensor 2
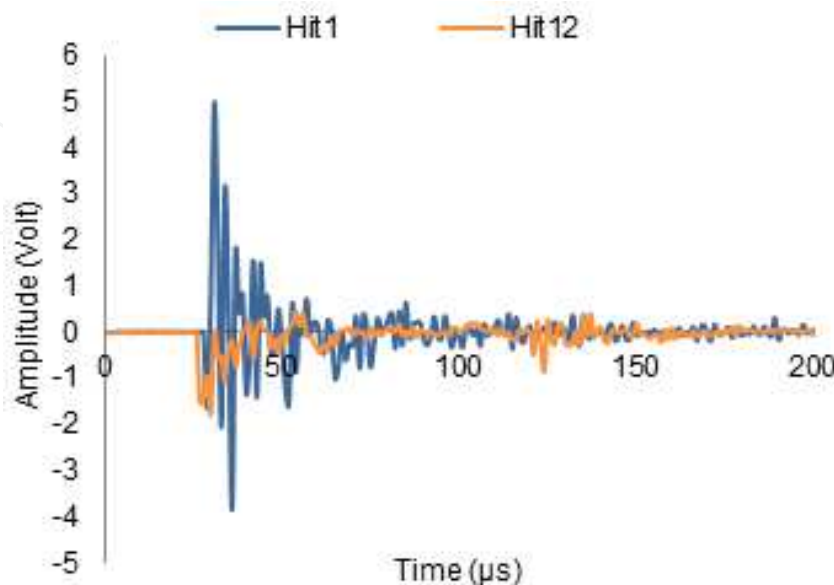

Figure 4. AE waveform for two different AE amplitudes during sensitivity checking

Generally, each PLF produces one signal of AE hit or more and in various form or shape of waves. Figure 4 shows different shapes of wave for two hits of PLF from Sensor 1. Hit 1 is a response of PLF that produces amplitude 99 dB and generates high peak wave. Hit 12 is for amplitude 91 dB response from the bounce back of the lead during PLF process and produced lower amplitude. Hit 1 generates high peak wave rather than Hit 12. Figure 3a indicated that Hit 12 occurred at the same time of PLF with other amplitudes. However, for sensitivity checking this will be ignored. The peak signal amplitude can be related to the intensity of the source in the material [21, 25]. Pullin et al. [26] stated that the good sensitivity between sensor and beam surface is enough when the amplitude signal exceeded 95 dB. Hence, sensitivity checking would be better when a higher amplitude is being produced during replicates of PLFs.

3.2. Identification of Time of Arrival (TOA)

Typical AE waveform parameter received by Sensor 1 type R6I from a 150 x 150 x 750 mm RC beam during PLF process, represented in amplitude (v) against time (µs) is shown in Figure 5. As lead breaks (in-plane or out-of-plane) on the surface of the beam, a wave propagates through a solid medium; it carries certain amount of energy. The energy can be consumed by scattering during propagation. The scattering effect principally relies on the defects such as micro-cracks inside the material. In wave velocity determination only several AE parameters would be considered such as time and amplitude. AE amplitude gives the information about the time at which AE signals take place [27]. Wave velocity is one of the methods to be considered for source location. Figure 6 presents the wave of the signal for threshold 40 dB. The first wave crosses the threshold level is known as P-wave.
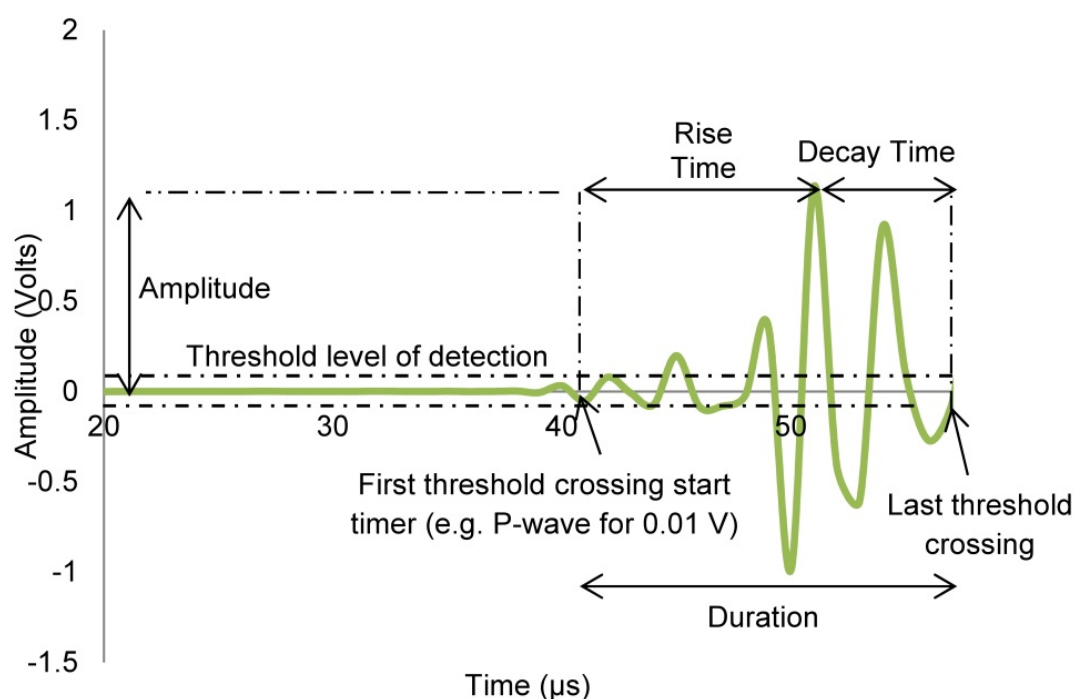

Figure 5. Simple waveform parameter

In this experiment, Sensor 1 was set as individual due to close to the AE source and the rest were considered as synchronize. For instance, the threshold was set at 40 dB prior to test. The Sensor 1 would be the first received the waves emitted by PLF at AE source followed by other sensors as depicted in Figure 6. In this figure, the TOA or longitudinal wave (P-wave) for Sensors 1, 2 and 3 were noted as t_1, t_2 and t_3 respectively. The AE signal for first P-wave, t_1 was examined out to 29 µs after the source initiation time followed by P-wave, t_2 for sensor 2 about 34 µs and P-wave for t_3 is 43 µs. In the test, gain 0 dB and preamplifier 40 dB were used with the sample interval of 10µs. In this case, the thresholds were assumed to be as lower as 40 dB (0.01V) to 70 dB (0.32V). Referring to eq. 1 and eq. 2, amplitude (represented in dB) can be calculated with the V_{ref} equals 1µv. Then, volt for each threshold levels can be determined. Volt for each threshold can be used as a guideline determine the TOA or P-wave at each sensor from AE source.
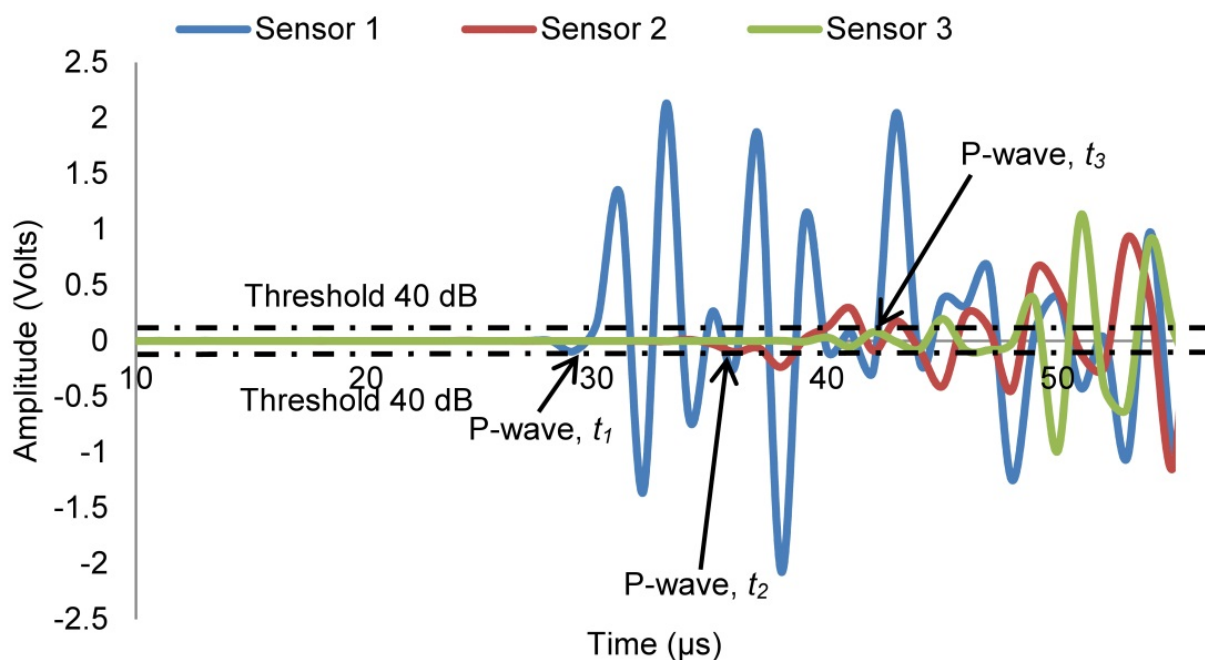

Figure 6. TOA or P-wave for threshold 40 dB at time 35.53 s for each sensor

3.3. Relationship between wave velocity and sensor distance for RC beam

The first method in the determination of wave velocity in 150 mm x 150 mm x 750 mm and 100 mm x 100 mm x 500 mm RC beam is based on the changes of pre-set threshold level in AE hardware or threshold crossing technique. Four different pre-set threshold levels were chosen namely 40 dB (0.01V), 45 dB (0.02V), 65 dB (0.2V) and 70 dB (0.32V). For each pre-set threshold level, 10 replicates of PLF were carried out in-plane and out-of-plane sources. TOA to each sensor for each PLF was analysed and followed by other replicates of PLFs. Figure 7a shows the relationship between the average wave velocity and sensor distance for out-of-plane source at each threshold level. Figure 7b presents the relationship of average wave velocity and sensor distance for in-plane source. Both figures show the wave velocities are apparently depends on the sensor distance and threshold levels.

In determination of wave velocity, sensors 1, 2 and 3 was set of 0 m, 0.2 m and 0.4 m, respectively. Figure 7 illustrates that, for RC beams 150 mm x 150 mm x 750 mm with sensor distances 0.2 m, at lower threshold level (40 dB) and higher threshold level (70 dB) for out-of-plane source, the velocity is in the range of 7889 m/s to 4559 m/s and 2409 m/s to 1654 m/s, respectively. Meanwhile in in-plane source, velocties for lower threshold and higher threshold are in the range of 3086 m/s to 2608 m/s and 2619 m/s to 2192 m/s, respectively. It is found that the wave velocity for in-plane source has lower velocity than out-of-plane source. It might be due to the in-plane source location is parallel to the sensor surface and the wave propagates take longer time to reach the sensors. Hence, the source location in linear measurement of sensors for in-plane would prolong the TOA of the wave to reach the sensor and the velocity is reduced. Out-of-plane source is longitudinal to the sensor surface and hence the wave signal propagates inside the RC beam take shorter time to reach the sensors. Thus, it reduces the TOA of the wave to each sensor.

In wave velocity calculation for beam 100 mm x 100 mm x 500 mm, sensors 1, 2 and 3 was set as 0, 0.1 m and 0.2 m, respectively. Figure 8 presents the wave velocity in 100 mm x 100 mm x 500 mm with sensor distances of 0.1 m for out-of-plane. The figure shows that the lower threshold level is in the range of 3430 m/s to 2810 m/s and the higher threshold level is 2765 m/s to 1166 m/s. Velocity propagates in in-plane source is in the range of 5030 m/s to 3150 m/s for threshold 40 dB and 2751 m/s to 2603 m/s for threshold 70 dB. In this case, apparently the velocity in the in-plane source has higher velocity than out-of-plane source. Logically, the pattern of the wave velocity occurred in the both size of beams with different spacing of sensors should be synchronized. However, this phenomenon indicates that the wave velocity in the RC beam or heterogeneous material cannot be predicted.
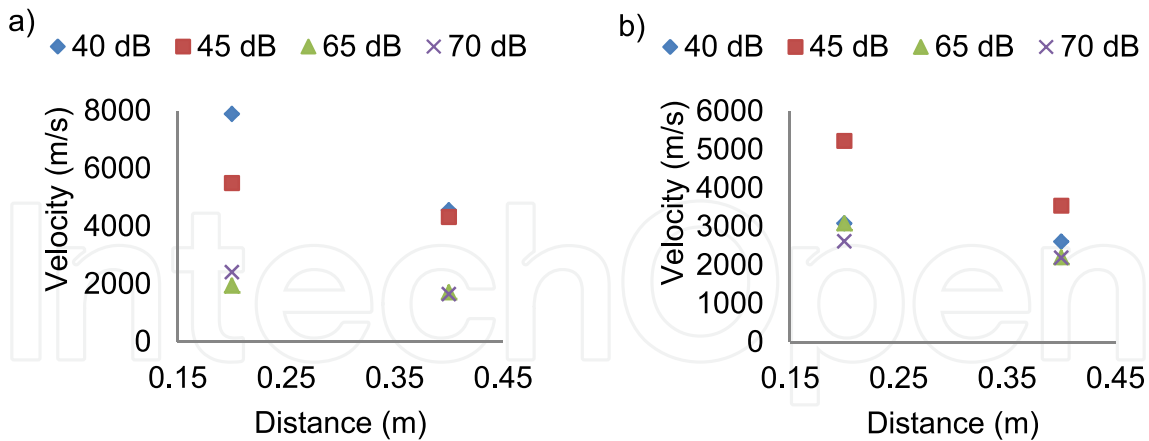

Figure 7. Wave velocity in 150 mm x 150mm x 750 mm RC beam for a) out-of-plane source and b) in-plane source

The results of the study were also compared to other research done in heterogeneous material as well as RC structure of the wave velocity of RC beam 100 mm x 150 mm x 2000 mm with the sensor distance of 250 mm, the value was in the range of 4000 m/s to 4500 m/s [3]. For large spectrum with frequency between 50 to 600 kHz, the wave velocity is 2350 m/s [28]. The wave velocity in ceramic matrix composite was 3200 m/s with the threshold level

of 48 dB; however, the initial velocity was 10000 m/s [29]. If resonant sensor of 300 kHz was used, the wave velocity is 4000 m/s [30]. For carbon fibre reinforced polymer (CFRP) the wave velocity equal to 1000 m/s [13].
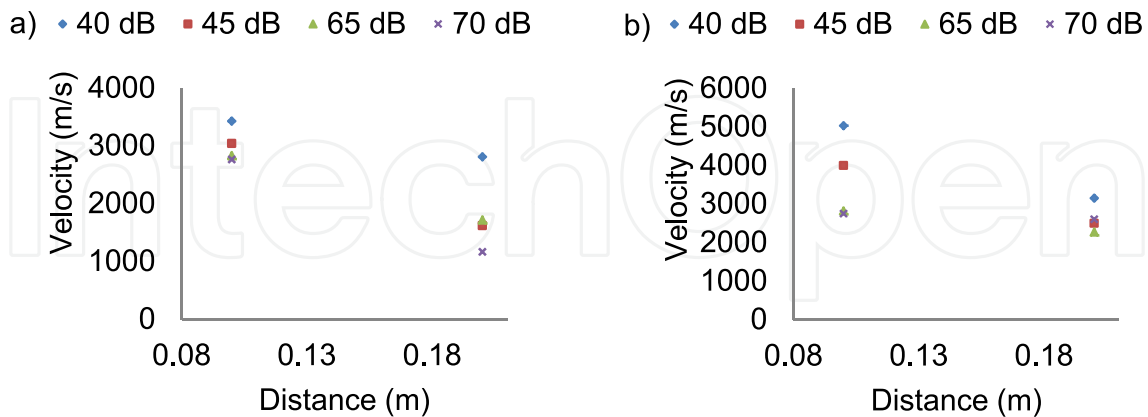

Figure 8. Wave velocity in 100 mm x 100 mm x 500 mm RC beam for a) out-of-plane source and b) in-plane source

3.4. Relationship between wave velocity and threshold level

Figures 9a and 9b display the velocity propagates in the 150 mm x 150 mm x 750 mm RC beam as threshold levels increased for out-of-plane and in-plane sources. As mentioned earlier, apparently the wave velocities depend on the threshold levels. Thus, the statistical coefficient can be used to enhance the prediction by identification of determination coefficient, R^2. For out-of-plane source, for sensors distance 0.2 m (Sensor 3-2), the R^2 is 91.3 % and for distance 0.4 m (Sensor 3-1) produced higher R^2 of 97.8 %. Thus, both distances have strong correlation between velocities and also the threshold level, where, the wave velocity in the RC beam is influenced by the threshold level crossing. The higher the threshold level, the lower of the wave velocity would be.

For in-plane source, distance between Sensors 1 to 2 and 1 to 3 is 0.2 m and 0.4 m, respectively. It is found that for in-plane source, both distances of sensors have weak correlation of 30.3 % for Sensors 1-2 and 49 % for Sensors 1-3. It is due to the wave velocities for 40 dB are lower than for threshold 45 dB with the approximate different in the range of 2100 m/s to 940 m/s. However, after threshold of 45 dB, the wave velocity seems has good correlation, which the threshold increased as the wave velocity decreased.

Figure 10 shows the relationship between wave velocity propagation and threshold level for 100 mm x 100 mm x 500 mm RC beam. Wave velocity for closet distance in Figure 10 shows a good relationship between velocity and threshold levels with the correlation of 83 % and 92 % for out-of-plane and in-plane source, respectively. However the longer distance represents a weak relationship with the correlation of 59 % and 40 % for out-of-plane and in-plane source, respectively. Overall the prediction of the wave velocity in short distance is influenced by threshold levels has strong correlation. However, for longer distance, the relationship is seemingly unpredictable.
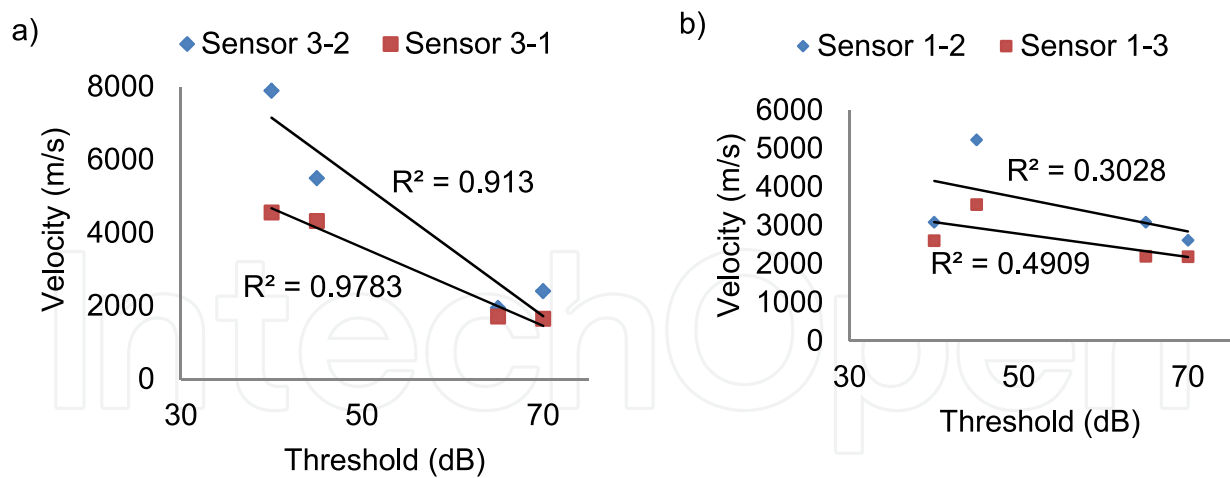
Figure 9. Relationship between velocity and threshold level on RC beam 150 mm x 150 mm x 750 mm for a) out-of-plane source and b) in-plane source
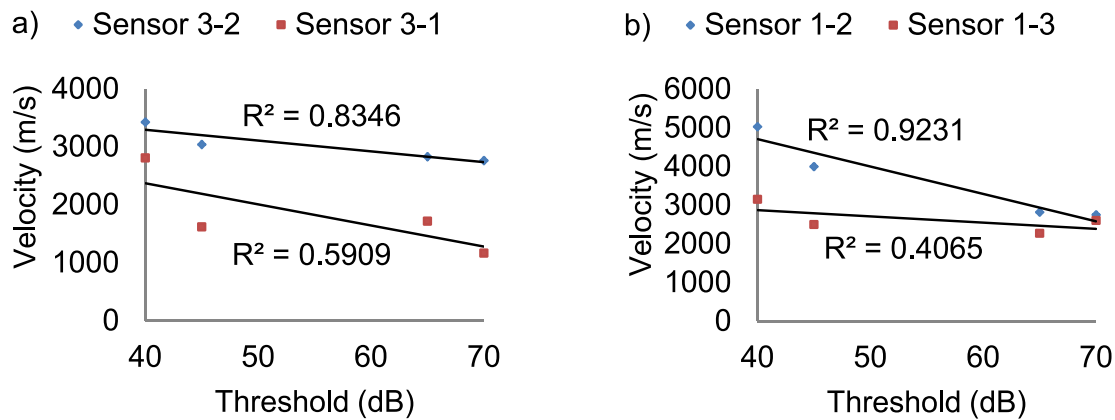

Figure 10. Relationship between velocity and threshold level on RC beam 100 mm x 100 mm x 500 mm for a) out-of-plane source and b) in-plane source

It can be concluded that the relationship of the velocity and threshold level is easy to predict for shorter distance, where the velocity decreases when the threshold level increases. It apparently indicates a good correlation for shorter distance. However, for longer distance the relationship is unpredictable and has weak relationship. This can be related with the material applied, where concrete always has imperfection of the composition such as voids.

3.5. Relationship between arrival time and sensor distance

Figure 11 shows the average of arrival time (μs) against sensor distance for original signal and corrected signal for out-of-plane source at threshold 40 dB, 45 dB, 65 dB and 70 dB on 150 mm x 150 mm x 750 mm RC beam. In the graphs, Cor stands for corrected signal and Ori stands for original signal. The corrected signal has been used to justify the correlation between TOA and distance. Sensor 3 (distance zero) close to the AE source, it receives the first TOA emits by PLF and follows by the other sensors. Sensor 1 would receive the last signal with the higher TOA. In some situation, the farthest sensors from the AE source

would not receive any signal. This phenomenon occurs because wave attenuation in the RC beam cannot be avoided. Wave attenuation is loss of AE energy as waves travel through in a material [25]. It is also the loss of amplitude with distance as the wave travel through the beam [7]. This is also affected of the time taken path of the signal wave from the AE source to the sensors. The farthest sensor would receive the lower signal wave and hence take longer TOA. For instance, Original 40 dB at fist sensor is 29 μs and the farthest sensor is 40 μs. Thus, TOA takes longer time to reach sensor 1. Other factor causes the waveform amplitude loss such as intrinsic mechanisms and imperfections. It is because the intrinsic mechanism (thermal effects) and imperfections (void and misoriented grains) reduce the amplitude of the wave by using scattering and reflections [4]. Otherwise, RC beam is a heterogeneous material; many obstacles such as aggregates and bars affected to the movement of waves and yet delayed the TOA to the longest distance from the AE source. If the attenuation is too large or size of the structure is too big, the location of the hit cannot be defined. Thus, the attenuation depends on the types of material through which the waves are progressing and the source of the waves [7].
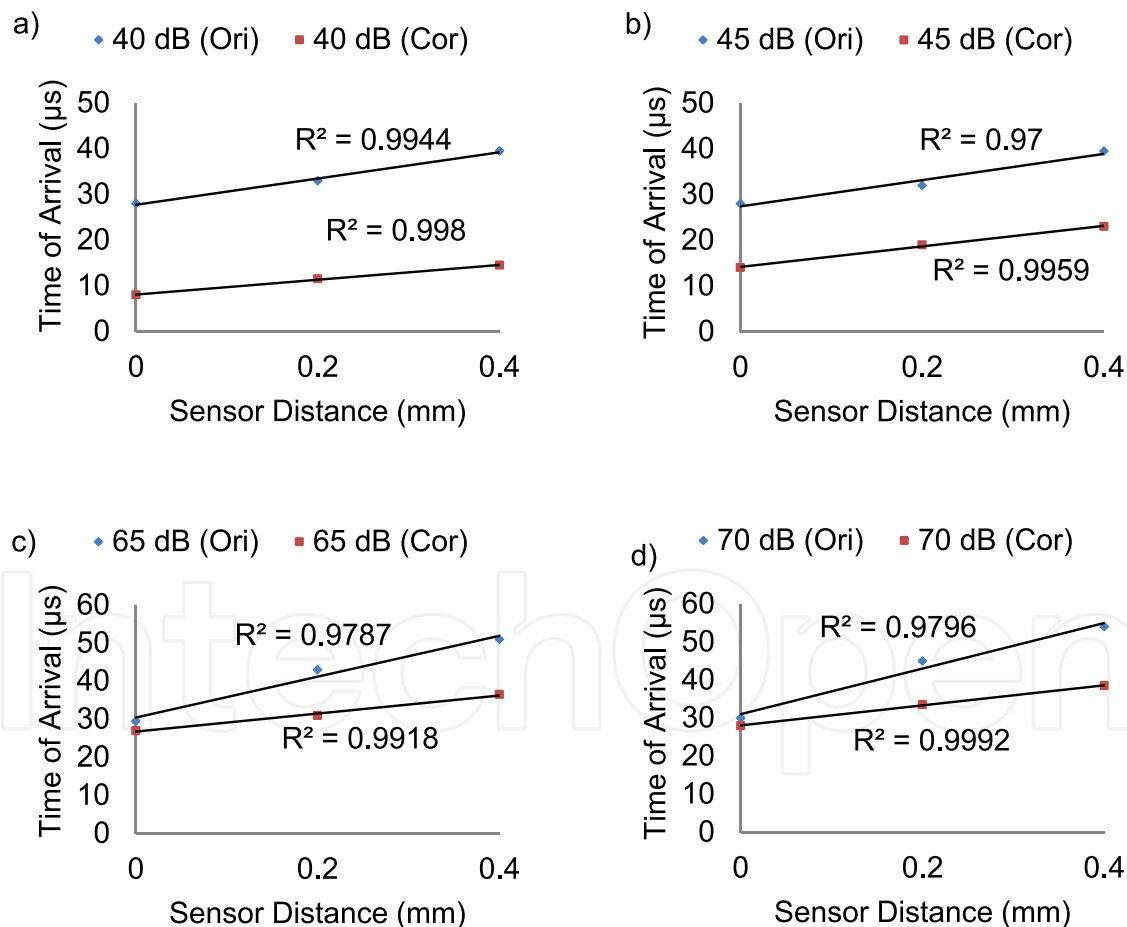

Figure 11. Regression analysis of arrival time against sensor distance for 150 mm x 150 mm x 750 mm RC beam (out-of-plane source) at a) 40 dB, b) 45 dB, c) 65 dB and d) 70 dB

All figures show very good correlation between TOA and sensor distance for out-of-plane source and there is insignificant difference between original signal and corrected signal. All

threshold levels have strong correlation with the determination of coefficient more than 97 % between TOA and sensor distance.

Figures 12 a), b), c) and d) represent the regression analysis of arrival time against sensor distance for in-plane source at threshold 40 dB, 45 dB, 65 dB and 70 dB, respectively. Similar to the one represented in Figure 11, it shows that all threshold levels have good correlation between time of arrival (TOA) and sensor distance with all the coefficient of determinations more than 96 %. However, threshold level of 40 dB for corrected signal analysis apparently has a perfect fit of linear correlation by representing the coefficient equal to 1. The value indicates that the TOA is absolutely influenced by the sensor distance. Similar to out-of plane source, the relationship also indicates no significant difference between original signal and corrected signal.

Figure 13 represents the regression analysis of TOA against sensor distance for 100 mm x 100 mm x 500 mm in-plane source at all threshold levels. Similarly, it shows that it has good correlation with the regression above 80 % with no significant difference between original signal and corrected signal.
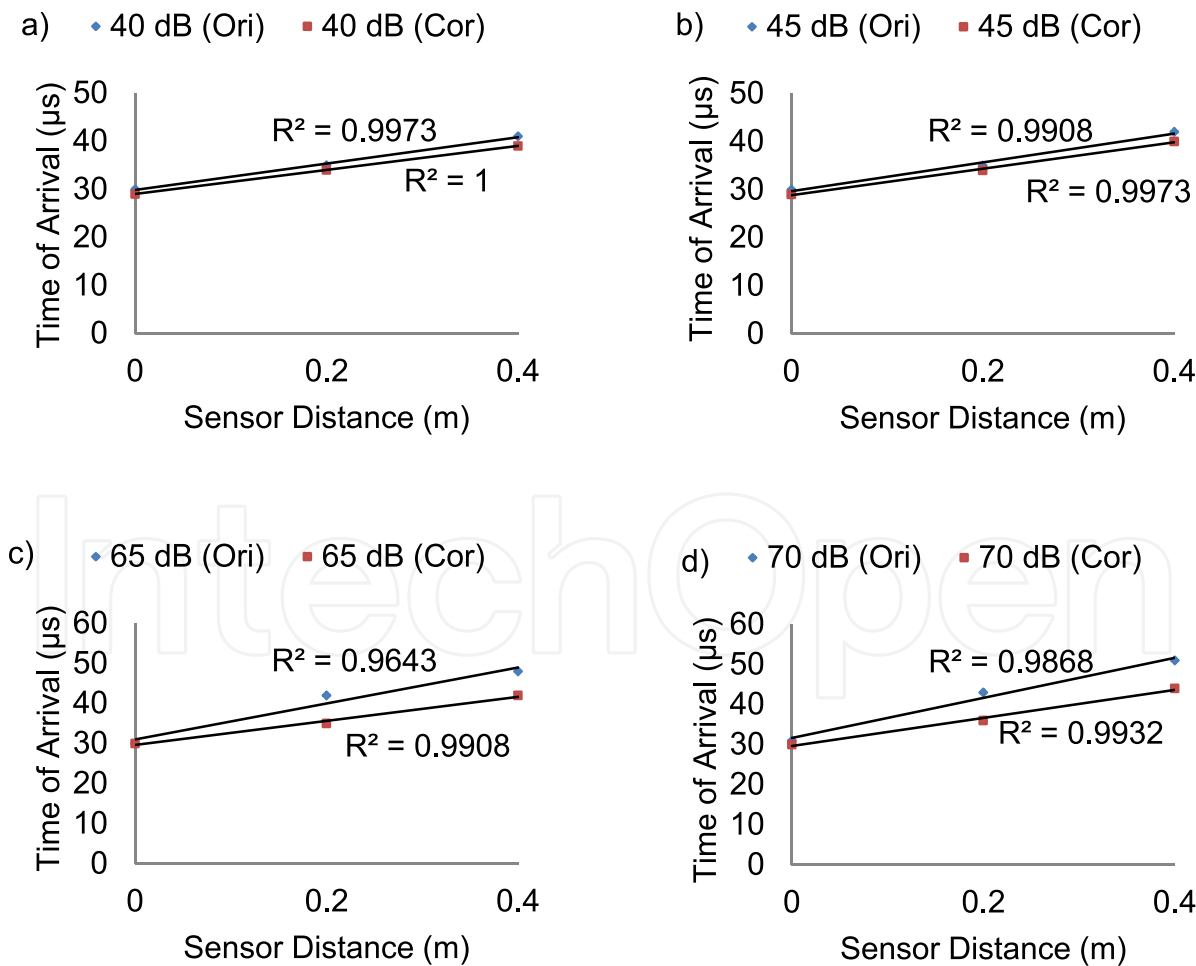

Figure 12. Regression analysis of arrival time against sensor distance for 150 mm x 150 mm x 750 mm RC beam (in-plane source) at a) 40 dB, b) 45 dB, c) 65 dB and d) 70 dB

Overall, the TOA of the wave propagation has good agreement with distance of sensors, where the longer the distance, the higher the time taken to reach the sensor. It can be seen in Figures 8 and 9, the slope of the best straight line drawn through the points are linear. However, other researchers found the relationship between TOA and sensor distance is not linear [3]. Since, the TOA is a good indication of wave velocity travels in the beam, hence the wave velocity decreases as the TOA increases.
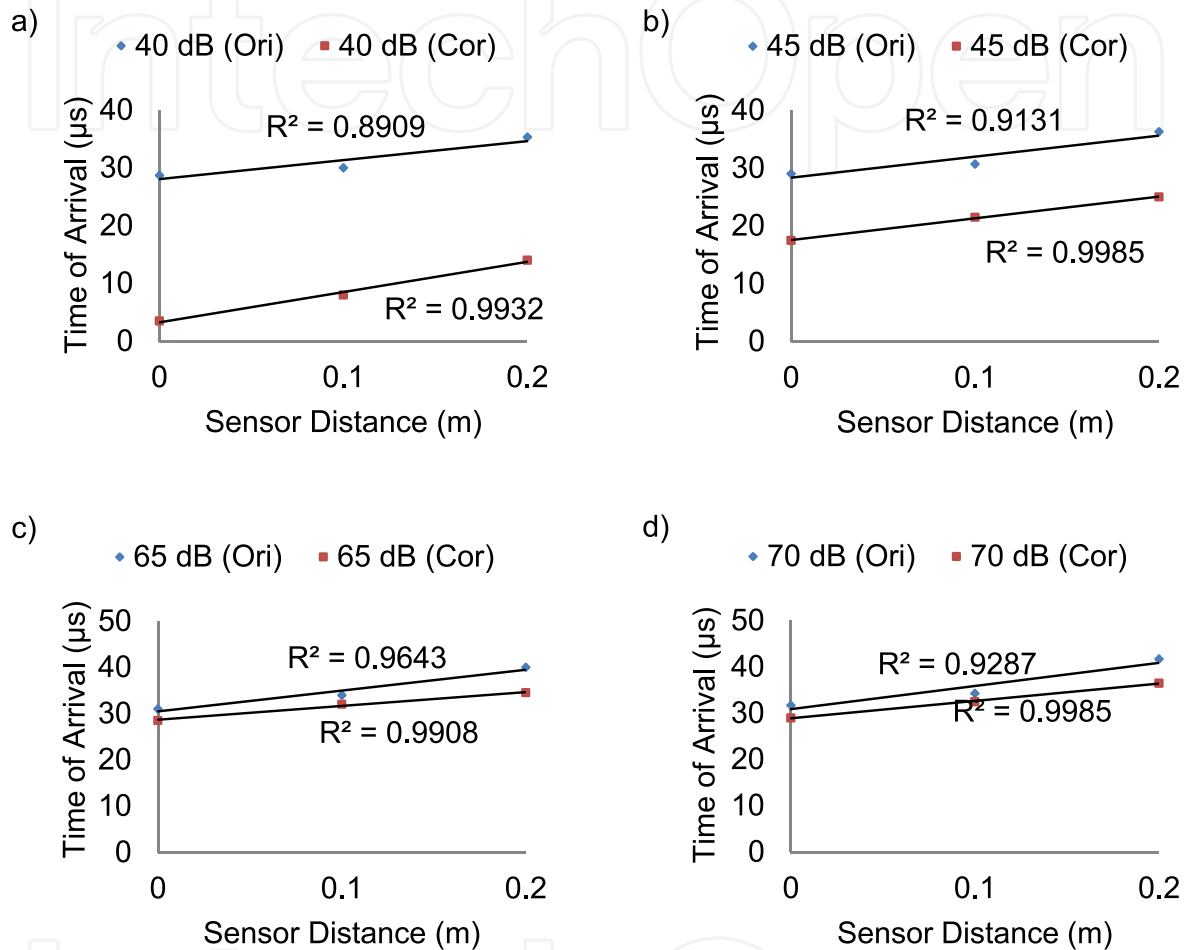

Figure 13. Regression analysis of arrival time against sensor distance for 100 mm x 100 mm x 500 mm (in-plane source) at a) 40 dB, b) 45 dB, c) 65 dB and d) 70 dB

4. Conclusions

Three sensors were used to determine the TOA and the wave velocity in RC beams. Sensor 1 was set as individual since it is close to the AE source and the first to receive the waves (P-Wave) that were emitted by PLF in the solid medium of concrete.

It can be concluded that AE wave velocities were found dependent on threshold levels and distance of sensor. It is found that the higher the threshold levels, the lower the wave velocity. This is because the threshold level prolonging arrival times of the waves and reducing velocities. Wave velocities for 150 mm x 150 mm x 750 mm were calculated to be in the range of 7889 m/s to 1654 m/s for out-of-plane source and 5229 m/s to 2192 m/s for in-

plane source. Wave velocities for 100 mm x 100 mm x 500 mm were computed to be in the range of 3430 m/s to 1166 m/s for out-of-plane source and 5030 m/s to 2603 m/s for in-plane source. Wave velocities decreases with the increasing distance between sensors and threshold levels. It was enhanced by the relationship of wave velocities and sensor distance for each threshold level.

The relationship between wave velocity and threshold level were identified for each sensor distance and then the coefficient of correlation, R^2 was determined. It is found that R^2 for beam 100 mm x 100 mm x 500 mm at out-of-plane source has good correlation than in-plane source. Beam 150 mm x 150 mm x 750 mm has weak correlation for longer sensor distance, but it has good correlation for shorter distance.

The relationship of TOA and sensor distance was identified. Its correlation was presented for each original signal and corrected signal. In total, both original signal and corrected signal indicated strong correlation between TOA and sensor distance with domain regression of 90 %.

Author details

Noorsuhada Md Nor and Soffian Noor Mat Saliah
Faculty of Civil Engineering, Universiti Teknologi MARA (UiTM), Permatang Pauh, Pulau Pinang, Malaysia

Norazura Muhamad Bunnori and Shahiron Shahidan
School of Civil Engineering, Engineering Campus, Universiti Sains Malaysia (USM), Seri Ampangan, Seberang Perai Selatan, Nibong Tebal, Pulau Pinang, Malaysia

Azmi Ibrahim and Hamidah Mohd Saman
Faculty of Civil Engineering, Universiti Teknologi MARA (UiTM), Shah Alam, Selangor, Malaysia

Acknowledgement

5. References

[1] ASTM E 1316-06 (2006) Standard Terminology for Non-Destructive Examinations. ASTM International, 5.
[2] Theobald P, Dar F (2006) AE Sensor Calibration for Out-of-Plane and In-plane Displacement Sensitivity. Advanced Materials Research. 13–14: 91–98.

[3] Muhamad Bunnori N, Pullin R, Holford KM, Lark RJ (2006) A Practical Investigation into Acoustic Wave Propagation in Concrete Structures. Advanced Materials Research. 13–14: 205–212.

[4] Ervin BL (2007) Monitoring Corrosion of Rebar Embedded in Mortar using Guided Ultrasonics Waves. PhD Thesis, University of Illinois, Urbana-Champaign.

[5] Liu Z (2007) Evaluation of Reinforced Concrete Beams using Cyclic Load Test, Acoustic Emission and Acousto-Ultrasonics. PhD Thesis, Auburn University, Auburn Alabama.

[6] Lovejoy S (2006) Development of Acoustic Emissions Testing Procedures Applicable to Conventionally Reinforced Concrete Deck Girder Bridges Subjected to Diagnoal Cracking. PhD Thesis, Oregon State University.

[7] ARCHES (2009) Sustainable Development, Global Change and Ecosystems Sustainable Surface Transport. ARCHES.

[8] Kurz JH, Köppel S, Linzer LM, Schechinger B, Grosse CU (2008) Source Localization. In: Grosse CU, Ohtsu M, editors. Acoustic Emission Testing. Springer. pp. 101–147.

[9] Grosse CU, Linzer LM (2008) Signal-Based AE Analysis. In:Grosse CU, Ohtsu M, editors. Acoustic Emission Testing. Springer. pp. 53–99.

[10] Zein, Abd-Elbaky AS (2005) Nondestructive Evaluation of Reinforced Concrete T-Shaped Beams by Frequency Spectrum Analysis of Impact-Echo Waveforms. PhD Thesis, University of South Carolina.

[11] Hamstad MA (2006) Contrasts between the Acoustic Emission Signals Generated by Monopole versus Dipole Sources. Advanced Materials Research, 13–14: 61–68.

[12] Gorman MR, Prosser WH (1991) AE Source Orientation by Plate Wave Analysis. Journal of Acoustic Emission. 9: 283-288.

[13] Degala S, Rizzo P, Ramanathan K, Harries KA (2009) Acoustic Emission Monitoring of CFRP Reinforced Concrete Slabs. Construction and Building Materials. 23: 2016–2026.

[14] British Standard BS8110 Part 1 (1997) Structural use of Concrete: Part 1. Code of Practice for Design and Construction. British Standard Institution.

[15] ASTM E650-97 (2007) Standard Guide for Mounting Piezoelectric Acoustic Emission Sensors. ASTM International, Pennsylvania United State.

[16] ASTM E976-10 (2010) Standard Guide for Determining the Reproducibility of Acoustic Emission Sensor Response. ASTM International. 5.

[17] Md Nor N, Muhamad Bunnori N, Ibrahim A, Shahidan S, Mat Saliah SN (2011) An Investigation on Acoustic Wave Velocity of Reinforced Concrete Beam In-Plane Source. 7th International Colloquium on Signal Processing and its Application. IEEE. 19–22.

[18] Chotickai P (2001) Acoustic Emission Monitoring of Prestressed Bridge Girders with Premature Concrete Deterioration. Thesis of Master Science in Engineering, The University of Texas, Austin.

[19] Physical Acoustic Corporation (2005) Samos AE System; Use's manual. Princeton Junction, NJ.

[20] ASNT (1996) Nondestructive testing handbook 2nd edition. Columbus, OH: American Society for Nondestructive Testing.

[21] Xu J (2008) Nondestructive Evaluation of Prestressed Concrete Structures by means of Acoustic Emissions Monitoring. PhD Thesis, Auburn University, Auburn, Alabama.

[22] Kalyanasundaram P, Mukhopadhyay CK, Subba Rao SV (2007) Practical Acoustic Emission. Indian Society for Non-Destructive Testing – National Certification Board Series.

[23] Baron JA, Yip SP (1987) Acoustic Emission Source Location. In: Miller RK, McIntire P, editors. Nondestructive Testing Handbook, 2nd edition Vol 5. American Society for Nondestructive Testing.pp.135-154.

[24] Qin L, Huang S, Cheng X, Lu Y, Li Z (2009) The Application of 1-3 Cement Based Piezoelectri Transducers in Active and Passive Health Monitoring for Concrete Structures. Smart Materials and Structures. 18: 1-8.

[25] Spanner JC, Brown A, Robert Hay D, Mustafa V, Pollock A (1987) Fundamentals of Acoustic Emission Testing. In: Miller RK, McIntire P, editors. Nondestructive Testing Handbook, 2nd edition Vol 5. American Society for Nondestructive Testing.pp.11-42.

[26] Pullin R, Theobald P, Holford KM, Evans SL (2006). Experimental Validation of Dispersion Curves in Plates for Acoustic Emission. Advanced Materials Research. 13-14: 53-60.

[27] Ni QQ, Jinen E (1997) Fracture Behaviour and Acoustic Emission in Bending Tests on Single-Fiber Composites. Engineering Fracture Mechanics. 56: 779-796.

[28] Marrec LL, Chekroun M, Villain G, Abraham O, Rakotomanana L (2009) Analytical Study of the Sensitivity of Rayleigh Wave for the Non-Destructive Evaluation of Cover-Concrete. Non-Destructive Testing in Civil Engineering.

[29] Momon S, Moevus M, Godin N, R'Mili M, Reynaud P, Fantozzi G, Fayolle G (2010) Acoustic Emission and Lifetime Prediction During Static Fatigue Tests on Ceramic Matrix-Composite at High Temperature under Air. Composites: Part A. 41: 913-918.

[30] Roca LOY (1997) Acoustic Emission Examination of High Strength Prestressed Concrete Girders. Master of Science in Engineering. The University of Texas, Austin.